Transp Porous Med (2015) 109:201–216
DOI 10.1007/s11242-015-0509-6

Wettability Alteration of Reservoir Rocks from Liquid Wetting to Gas Wetting Using Nanofluid

Morteza Aminnaji[1] · Hossein Fazeli[1] · Alireza Bahramian[1,2] · Shahab Gerami[3] · Hossein Ghojavand[3]

Received: 30 July 2013 / Accepted: 9 May 2015 / Published online: 20 May 2015

Abstract Well productivity in gas condensate reservoirs is reduced by condensate banking when the bottom hole flowing pressure drops below the dew point pressure. Among the several methods which have been proposed for condensate removal, wettability alteration of reservoir rock to intermediate gas wetting in the near wellbore region appears to be one of the most promising techniques. In this work, we report use of a nanofluid to change the wettability of the carbonate and sandstone rocks to intermediate gas wetting. Application of nanofluid in the wettability alteration of carbonate and sandstone rocks to gas wetting has not been reported previously and is still an ongoing subject. Static and dynamic contact angle measurements, along with imbibition tests, have been performed to investigate the wettability of carbonate and sandstone rocks in presence of nanofluid. It was found that the nanofluid used in this work can considerably change the wettability of both surfaces to preferentially gas wetting in just one day of ageing time. We also report the effect of initial oil saturation and ageing time on the nanofluid capability for wettability change. Initial oil saturation reduces the impact of the nanofluid on wettability change, and hence, a pre-treatment before using nanofluid is necessary. In addition to these small slab-scale experiments, applicability of nanofluid in wettability alteration of sandstone rocks to gas wetting is also investigated in core scale. The results of core displacement tests confirm the ability of nanofluid to change the rock wettability from liquid wetting to gas wetting in core samples. They also show the effectiveness of chemical treatment in subsurface conditions.

Keywords Gas condensate reservoirs · Condensate blockage · Nanofluid · Wettability alteration · Gas wetting

✉ Alireza Bahramian
abahram@ut.ac.ir

1 Institute of Petroleum Engineering, University of Tehran, P.O. Box 11155-4563, Tehran, Iran

2 Department of Chemical Engineering, University of Tehran, P.O. Box 11365-4563, Tehran, Iran

3 NIOC Research & Development, Negar St., Valiasr St., Tehran, Iran

List of symbols

T	Time after contact
M	Mass of liquid absorbed on solid
C	Material constant characteristic of solid sample

Greek letters

γ	Surface tension
θ	Contact angle
ρ	Density of liquid
μ	Viscosity of liquid

Subscripts

s	Solid
l	Liquid
a	Advancing
r	Receding

1 Introduction

Gas condensate reservoirs represent an important source of hydrocarbon reserves. Typically, such reservoirs are single-phase gas at original reservoir condition, but during their production life, reservoir pressure decreases, and below the saturation pressure, the fluid separates into two phases, a gas and a condensate liquid which then becomes trapped by capillary forces. The condensate saturation in the near wellbore region can reach 40–60 % (Whitson et al. 1999). This phenomenon, known as condensate banking or condensate blockage, results in reduced gas relative permeability and lowered well deliverability. Water blockage also lowers gas relative permeability (El-Banbi et al. 2000) and increases the impact of liquid blockage on the well deliverability.

Several treatment options exist for reducing condensate blockage and the impact of condensate saturation. Various solutions have been proposed, ranging from well re-completion to field-wide injection programs:

- re-perforating the wellbore, and solvent injection (Al-Anazi et al. 2005; Liangui et al. 2000; Alzate et al. 2006)
- dry gas injection (condensate re-vaporization) (Smith and Yarborough 1968; Shi et al. 2001)
- water injection, nitrogen injection to drive condensate back (Siregar et al. 1992)
- increasing reservoir contact using horizontal well (Muladi and Pinczewski 1999)
- hydraulic fracturing, and near wellbore wettability alteration are additional examples to mention

Apart from the wettability alteration method, other methods are not permanent solutions and the condensate bank will re-form (Li and Firoozabadi 2000a). The latter authors (2000b) studied the gas condensate system using a phenomenological network model and investigated

the effects of interfacial tension, gravity, flow rate, contact angle hysteresis and network size on the critical condensate saturation. Their studies showed that high gas well deliverability may be achieved by alteration of the near wellbore wettability to gas wetting and is the most effective method.

Li and Firoozabadi (2000a) were the first to report the wettability change of reservoir rock from liquid wetting to intermediate gas wetting by using fluoro-polymer chemicals, showing that oil recovery and phase relative permeability in a gas–oil system can be increased using the fluoro-polymer FC722. Further, it was verified that this chemical can be used successfully at temperatures up to 140 °C (Tang and Firoozabadi 2002, 2003).

Noh and Firoozabadi (2008) used an alcohol-based surfactant polymer solution to study the wettability alteration to intermediate gas wetting, with experimental results showing a considerable increase in water mobility. More recently, Wu and Firoozabadi (2010) demonstrated the permanency of the wettability alteration by providing a chemical reaction between rock and new chemicals having various functional groups.

In addition to the research conducted by Firoozabadi's group, other researchers have studied the wettability alteration to gas wetting. Kumar et al. (2006) evaluated surfactants in methanol–water mixtures to treat cores under reservoir conditions. Their experimental data indicated an increase in steady-state gas and condensate relative permeability. Adibhatla et al. (2006) studied behaviour of different surfactants to change wettability of reservoir rocks from water wetting to intermediate wetting. They found less water wetting in presence of chemicals with higher fluoro-group numbers. Li et al. (2011) developed a new and inexpensive chemical with sufficient stability at high temperatures, capable of increasing the gas- and water-phase relative permeability. Sharifzadeh et al. (2013) prepared a new polymer surfactant coating using a sol–gel process which was able to enhance the liquid repellency of the solid surfaces. Recently, Feng et al. (2012) synthesized a fluorine-containing, acrylate co-polymer emulsion by a cost-effective method, with reasonable capability to increase the gas wetting nature of the surface.

In this work, we study the wettability alteration of carbonate and sandstone rocks from liquid wetting to intermediate gas wetting, using a nanofluid. Nanofluids are suspensions of nanoparticles (nominally 1–100 nm in size) in conventional base fluids such as water, oils, or glycols, which have seen enormous growth in popularity (Taylor et al. 2013). To the best of our knowledge, use of nanofluids for wettability alteration of reservoir rocks to gas wetting has not been reported previously. We demonstrate wettability alteration using contact angle measurement and liquid imbibition test, with rock surfaces being characterized by use of EDX and SEM images. We also investigate the effects of initial *n*-decane saturation and ageing time in the nanofluid, on wettability alteration using the technique. Moreover, we study the effect of nanofluid on wettability alteration by a core displacement test to investigate the ability of the nanofluid in flow tests, which better represents reservoir conditions.

2 Material

Carbonate and sandstone rocks were used for the study of wettability alteration. In order to study the hydrophobicity and oleophobicity of the rocks, water and *n*-decane were used as the aqueous phase and oil phase, respectively. Air was used as the gas phase in contact angle measurements and core displacement tests. The porosity and permeability of sandstone rocks were 24 % and 190 md, respectively, with corresponding values for carbonate rocks of 20 % and 30 md. *SurfaPore M* nanofluid, manufactured by NanoPhos SA, was used to alter the wettability of carbonate and sandstone rocks, from strongly liquid wetting to intermediate gas

wetting. *SurfaPore M* is water based, with very low volatile organic compound (VOC) formulation, nano-structured emulsion of silicon-based molecules and fluoro-polymer, specifically designed to harness the power of nanotechnology, in order to achieve both oil and water repellency on the surfaces applied. Its viscosity and gravity are 2 cp (at 25 °C) and 1 g cm^{-3}, respectively. The active solid content of *SurfaPore M* is equal to 2 % w/w, containing a blend of different size nanoparticles to successfully modify slightly porous surfaces (such as marble or granites) and absorptive surfaces (such as cement or stones). Its unique formulation combines nanoparticles, partially coated with organofluorated coatings that provide water and oil repellency and resistance to extreme temperature ranges. Some key benefits of *SurfaPore M* are ability to withstand temperatures up to 350 °C, being water based, environmentally friendly, and cost-effective.

3 Experimental Methods

3.1 Small-Scale Slab Tests

3.1.1 Treatment Process

To perform contact angle and imbibition tests, carbonate and sandstone plates were first cut into small plates using a trimming machine and burnished with an end-face grinder to achieve a flat and relatively smooth surface. The dimensions of the rectangular sandstone samples were 2.4 cm × 2 cm × 0.3 cm. The circular carbonate samples had a radius of 1.8 cm and thickness of 0.3 cm. The plates were cleaned with toluene, then washed by distilled water and dried at 70 °C for 24 h. The dried samples were submerged in *SurfaPore M*, the nanofluid being used directly, without addition of any other chemical or water to it, and maintained at 70 °C for three days. The final samples were then dried at 70 °C for about 24 h, and the dried plates were used for contact angle measurements and imbibition tests. During the experiments, it was observed that the efficiency of *SurfaPore M* at ambient temperature is low, but increases significantly at higher temperatures.

3.1.2 Contact Angle Measurement

3.1.2.1. Static Contact Angle After placing the liquid droplet using a syringe on the untreated and treated rocks, static contact angle was measured by analysing the droplet image. Figure 1 shows the schematic of apparatus used for static contact angle measurement.

3.1.2.2. Dynamic Contact Angle In order to investigate dynamic contact angle, advancing and receding contact angles are measured. There are several techniques for measuring the advancing and receding contact angle, e.g. liquid injection or withdrawal through; lateral movement of substrate with the drop anchored to the needle; tilted plate; and the Wilhelmy method, which was the one chosen for measurement of dynamic contact angle. Demonstrated in Fig. 2, advancing and receding contact angles are measured by lowering a solid sample into liquid to a certain depth and then raising it, respectively. The force on the balance is given by:

$$F_{\text{total}} = \text{wetting force} + \text{weight of probe} - \text{buoyancy} \tag{1}$$

Here wetting force is defined as $\gamma_{\text{lv}} P \cos\theta$, where P is the perimeter of the plate. Dynamic contact angles may be measured at various speeds and should be equal to static contact angles at low velocities.

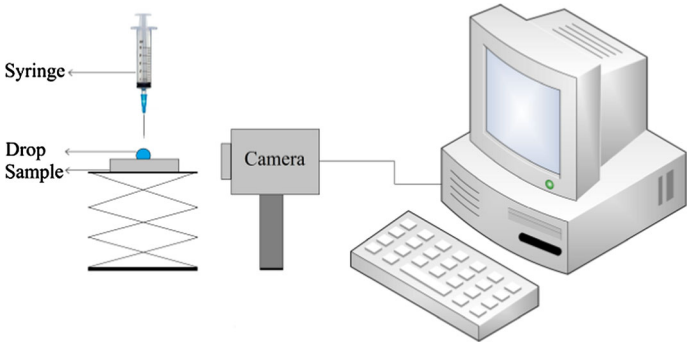

Fig. 1 Schematic for static contact angle measurement

Fig. 2 Schematic for dynamic contact angle measurement

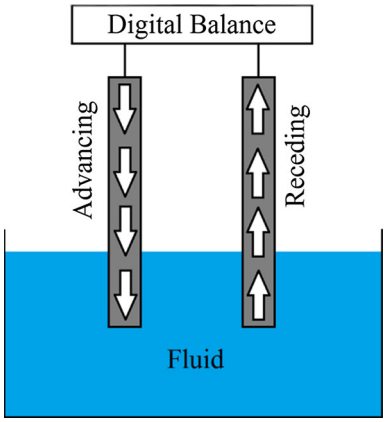

By measuring the advancing and receding contact angles, the total solid surface free energy can be calculated using the equation developed by Chibowski (2003);

$$\gamma_s = \gamma_l \left(\cos\theta_a + \cos\theta_r\right) \frac{(1+\cos\theta_a)^2}{(1+\cos\theta_r)^2 - (1+\cos\theta_a)^2} \tag{2}$$

Here, θ_a and θ_r are advancing and receding contact angles, and γ_l is the surface tension of the liquid.

3.1.2.3. Pseudo-contact Angle Penetration of liquid into the pores of the solid causes an error in measuring the force and hence in the dynamic contact angle. The Washburn method (Washburn 1921) is then used to evaluate the wettability in porous media, as according to the Washburn theory, when a porous medium contacts a liquid, the liquid rises into the solid, obeying the following relationship:

$$T = \left[\frac{\mu}{C\rho^2\gamma\cos\theta}\right] M^2 \tag{3}$$

Here, T is time after contact, μ is liquid viscosity, ρ is liquid density, γ is surface tension, θ is contact angle, M is mass of liquid absorbed in solid, and C is the material constant, characteristic of the solid sample, which may be related to the porosity and permeability of the porous material. 'C' can be readily measured using a liquid which wets the solid

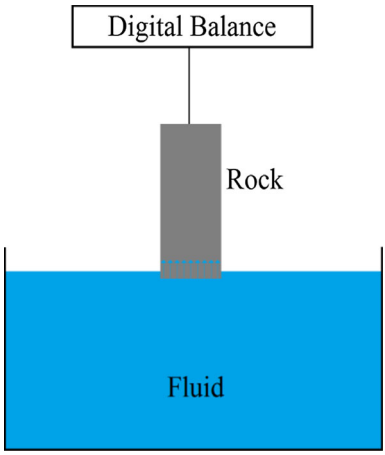

Fig. 3 Schematic for imbibition test

completely, such as *n*-hexane, as used in the tests here. In this case, the contact angle is zero. Tang and Firoozabadi (2002) used this method to evaluate wettability and called this contact angle as a pseudo-contact angle. It is obvious that pseudo-contact angle is between 0° and 90°, corresponding to completely wet and non-wet conditions, respectively.

3.1.3 Imbibition

An imbibition test can be performed to evaluate the effect of wettability on fluid imbibition into the porous media sample. The amount of liquid absorbed in a solid plate versus time was measured for a porous solid with different wettability characteristic, using a set-up shown in Fig. 3. There, it is clear that a liquid wet medium absorbs more liquid than one with a gas wetting nature.

It should be pointed out also that dynamic and pseudo-contact angle measurements and imbibition tests were performed using a Sigma 700 (KSV) as shown in Fig. 4, which is a state-of-the-art multipurpose force tensiometer that is able to perform a wide range of measurements and adapt to a great variety of experimental settings. The highly sensitive instrument offers high-precision surface and interfacial tension measurements; fully automated critical micelle concentration (CMC) determinations; and measurement of dynamic contact angle, surface free energy, powder wettability, sedimentation, and density. The technical specifications of Sigma 700 (KSV) can be found in Table 1.

3.2 Core Displacement Tests

Fluid flow tests were also conducted to evaluate the efficiency of nanofluid in wettability alteration in core scale. Figure 5 shows the schematic of the experimental set-up, where the sandstone core with a diameter of 3.75 cm and length of 12 cm was placed inside the core holder, and an overburden pressure of 800 psia was applied. The temperature of the system was maintained by an oven, and the pressure drop was measured by pressure transducers and recorded by a data acquisition system. The liquid flow rate was fixed using a pump.

Brine (KCl 2 %) was injected at a fixed flow rate of 2 cc/min into the untreated, air-saturated sandstone core, and the transient pressure drop recorded until the steady state was reached. After that, the core was dried in an oven at 70 °C, having first been evacuated to

Fig. 4 Sigma 700 (KSV)

Table 1 Sigma 700 (KSV) technical specifications

Sigma 700 (KSV)	
Available measurements	
Surface tension	√
Interfacial tension	√
Critical micelle concentration	Automatic
Dynamic contact angle	√
Surface free energy	√
Powder wettability	√
Density	√
Sedimentation	√
Balance specifications	
Measuring range (mN/m)	1…2000
Displayed resolution (mN/m)	0.001
Density range (g/cm^3)	0…2.2
Density resolution (g/cm^3)	0.0001
Maximum load (g)	210
Weighing resolution (mg)	0.01
Force resolution (μN)	0.1
Contact angle range (°)	0…180
Contact angle resolution (°)	0.01
Calibration and locking	Automatic

Table 1 continued

Sigma 700 (KSV)	
Measuring unit specifications	
Sample stage	Motorized
Sample stage speed (mm/min)	0.01…500
Stage movement range (mm)	0…75
Stage positioning resolution (μm)	0.016

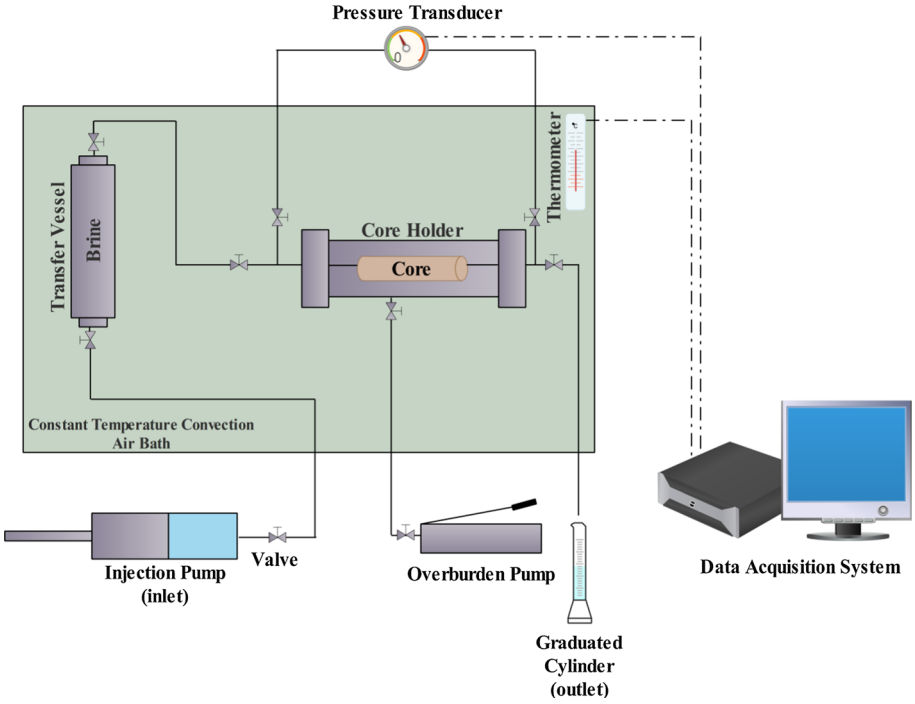

Fig. 5 Schematic of core flooding setup

draw in the nanofluid. Three pore volumes (PVs) of chemical solution was injected, followed by ageing for 1 day at 70 °C. Roughly, 20 PVs of brine was then injected to displace the chemical solution and wash the core. Both the injection of chemical solution and the brine were carried out at a flow rate of 2 cc/min, with air then injected at a pressure of 100 psia to drain the water from the core. Finally, the core was removed from its holder and dried in an oven at 70 °C. After the treatment process, brine was re-injected into the core to investigate the changes in the pressure drop.

4 Results and Discussion

4.1 Contact Angle Measurements

Static and dynamic contact angles of water and *n*-decane increased after coating the sample with nanofluid confirming that treated rock repels both fluids. As shown in Fig. 6, treatment

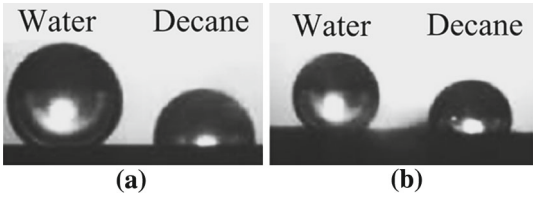

Fig. 6 Static contact angle for treated rocks. **a** Carbonate rock, **b** sandstone rock

Table 2 Static, advancing, receding, and pseudo-contact angles of water and *n*-decane, and surface free energy of untreated and treated carbonate and sandstone rocks

Sample	Carbonate rock				Sandstone rock			
	Untreated		Treated		Untreated		Treated	
	Water	*n*-Decane	Water	*n*-Decane	Water	*n*-Decane	Water	*n*-Decane
Static contact angle	58°	0°	139°	95°	0°	0°	138°	104°
Advancing contact angle	81°	0°	140°	107°	47°	0°	142°	106°
Receding contact angle	0°	0°	110°	90°	0°	0°	115°	43°
Pseudo-contact angle	0°	0°	90°	90°	0°	0°	90°	90°
Surface free energy (mN/m)	50.6		4.3	6.7	55.4		4.1	4.9

with *SurfaPore M* results in a water static contact angle of about 139° for treated carbonate and sandstone rocks. In contrast, the water static contact angles for untreated carbonate and sandstone rocks are 58° and 0°, respectively. Similar results have been obtained for *n*-decane static contact angles (Table 2). The contact angles for *n*-decane for treated carbonate and sandstone rocks are 95° and 104°, while *n*-decane completely wets (zero contact angle) the untreated carbonate and sandstone samples. According to these measurements, *SurfaPore M* has increased the static contact angle to a greater degree than the chemicals reported in previous studies.

Figure 7 shows the total force exerted on the treated and untreated carbonate and sandstone samples by the test liquids (water and *n*-decane) at different depths inside the liquid. As can be seen, in all cases the total force decreases as the immersion depth increases, the trend which is explained by the effect of buoyancy, which increases as the sample is lowered to the required immersion level, hence the reduction in the total force. By measuring the latter and buoyancy at each depth, the wetting force can be calculated using Eq. 1, enabling the contact angle to be calculated, i.e. the 'advancing contact angle' in this process. Conversely, the buoyancy force decreases in the reverse direction (withdrawal process), increasing the total force, enabling calculation of the 'receding contact angle'.

As it is evident from Fig. 7, the total force versus immersion depth curve for treated rock is lower than that for untreated rock, indicating that wetting force decreases after treatment, resulting in higher advancing and receding contact angles. The value of the total force will become negative after a specific immersion depth due to the increase in buoyancy force with immersion depth. The difference between advancing and receding contact angle curves which indicates the contact angle hysteresis increases after treatment. It is believed that the contact angle hysteresis is attributable to surface heterogeneity and surface roughness (Wenzel 1936; Cassie and Baxter 1944; Li and Amirfazli 2005). The formation of nanostructures on the rock surface is responsible for both heterogeneity and roughness of the surface, hence the increase in hysteresis.

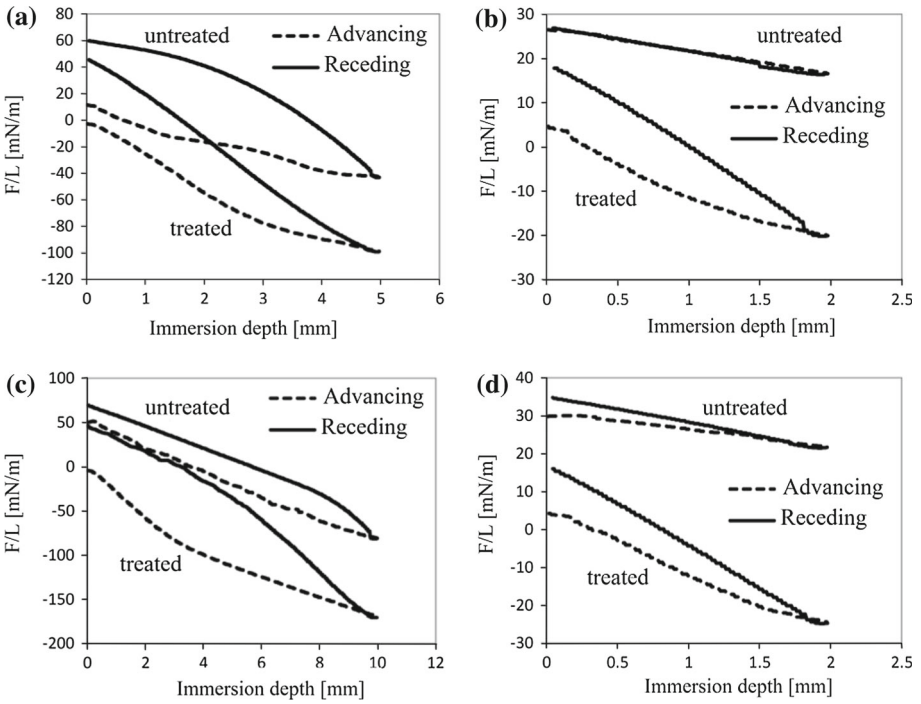

Fig. 7 Total force/wetted length of sample versus immersion depth for treated and untreated rocks. **a** Water imbibition into carbonate rock, **b** *n*-decane imbibition into carbonate rock, **c** water imbibition into sandstone rock, **d** *n*-decane imbibition into sandstone rock

Before measuring the pseudo-contact angle values, we should measure the material constant characteristic for treated and untreated rocks, which for carbonate rocks are 0.000073 and 0.000579 for untreated and treated, respectively. The corresponding values for sandstone rocks are 0.005881 and 0.02. Hence, there has been a considerable increase in the material constant characteristic after treatment. Using these measured values, the pseudo-contact angle increased from 0° (for untreated sample) to 90° (for treated sample) in all cases. All of the contact angle results which are summarized in Table 2 demonstrate the ability of nanofluid to alter wettability from liquid wetting to gas wetting.

4.2 Surface Characterization

In addition to surface roughness, surface free energy is the other parameter that affects the wettability. To have a gas wet surface with liquid repellent character, the surface free energy must be very small. Table 2 shows the values of surface free energy (about 4 mN/m for both treated surfaces) calculated by Eq. 2. This low surface free energy is due to the presence of organofluorinated chemicals within the nanofluid. It is noteworthy that trifluoromethyl group (CF_3) terminated surfaces possess low surface free energy of ~6 mN/m (Hsieh et al. 2011).

Figure 8 shows the SEM images of the treated and untreated carbonate and sandstone plates, clearly showing the formation of a film containing organofluorine and silicon-based nanoparticles. Moreover, Fig. 8c, f shows the fluorine and silicon 'map' on the carbonate and sandstone surfaces. EDX analysis of the samples aged in the nanofluid is shown in

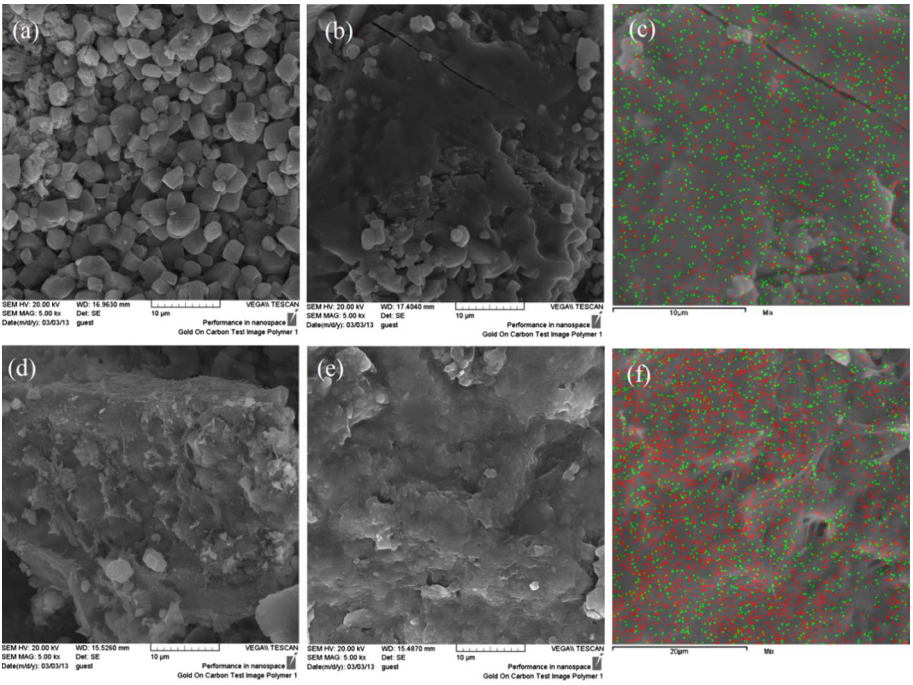

Fig. 8 SEM images. **a** Untreated carbonate rock, **b** treated carbonate rock, **c** EDX map of fluorine (*green points*) and silicon (*red points*) on the treated carbonate surface, **d** untreated sandstone rock, **e** treated sandstone rock, **f** EDX map of fluorine (*green points*) and silicon (*red points*) on the treated sandstone surface

Fig. 9. As is evident from this figure, the surfaces are composed of F and Si as constituent materials of the nanofluid. The untreated carbonate rock was mainly composed of Ca without F and Si elements, and hence, the presence of F and Si on the treated carbonate rock surface proves the adsorption of fluorine and silicone on the surface. Similar results were observed for sandstone rocks with the exception that the Si element was present in both treated and untreated sandstone.

4.3 Imbibition

Imbibition tests on the carbonate and sandstone plates were performed to study the wettability alteration to intermediate gas wetting using a Sigma 700 (KSV). Figure 10 shows the amount of liquid absorbed into solid plates versus time. As the Sigma 700 (KSV) can record the data every second, the data appear to be a continuous line. There was a sharp decline in liquid imbibition after treatment by nanofluid. Water imbibition in carbonate rock is illustrated in Fig. 10a, where the amount of water imbibed after 300 s is 0.159 and 0.007 PV for untreated and treated rock, respectively. The reduction of 95.6 % water imbibition in treated carbonate rock represents a successful alteration of wettability to gas wetting. Also a reduction in *n*-decane imbibition was obtained in treated carbonate rock. As shown in Fig. 10b, 0.032 and 0.007 PV of *n*-decane were imbibed into untreated and treated carbonate rock. The reduction of 79.2 % *n*-decane imbibition in treated carbonate rock was observed. This reduction was lower than that of water imbibition, which is in line with the measured contact angles of water and *n*-decane. Similar results were obtained for sandstone plates. The amount of water

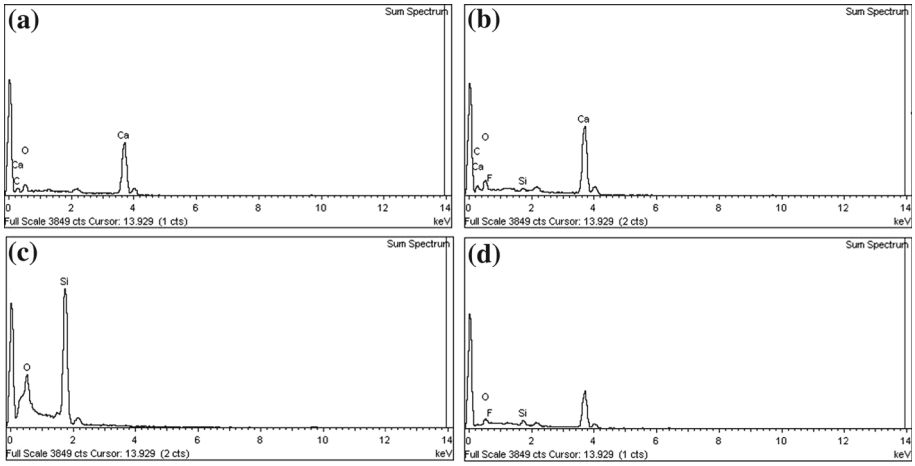

Fig. 9 EDX analysis of **a** Untreated carbonate rock, **b** treated carbonate rock, **c** untreated sandstone rock, **d** treated sandstone rock

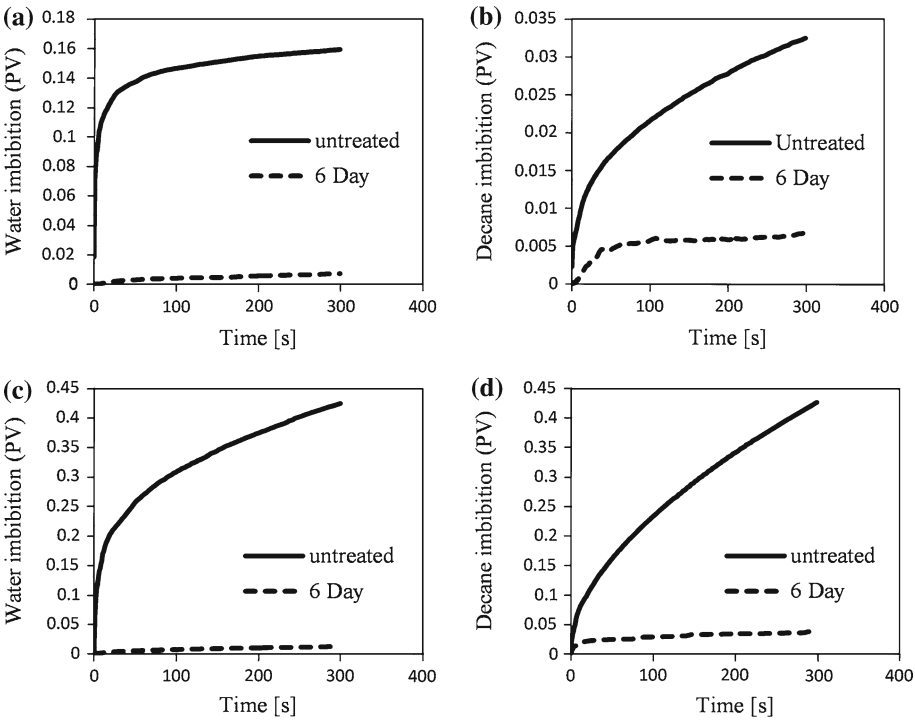

Fig. 10 Imbibition into the untreated and treated rocks at 25 °C and 1 atm. **a** Water imbibition into carbonate rock, **b** *n*-decane imbibition into carbonate rock, **c** water imbibition into sandstone rock, **d** *n*-decane imbibition into sandstone rock

imbibed into the sandstone rock was 0.425 and 0.013 PV for untreated and treated samples, respectively, as shown in Fig. 10c. Correspondingly, the values for *n*-decane imbibition were 0.426 and 0.039 PV (Fig. 10d).

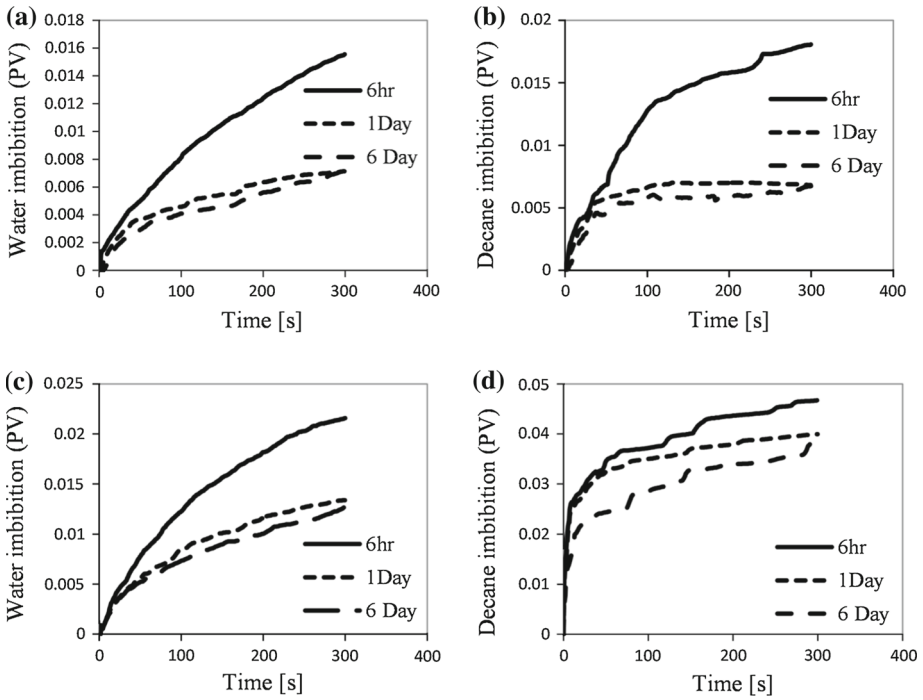

Fig. 11 Effect of different ageing times (6 h, 1 day, and 6 days) to treat rocks at 70 °C based on imbibition test. **a** Water imbibition into carbonate rock, **b** *n*-decane imbibition into carbonate rock, **c** water imbibition into sandstone rock, **d** *n*-decane imbibition into sandstone rock

The sharp decline in liquid imbibition after treatment was also observed in sandstone plates, with a reduction of 97.0 and 91.0 % evident for water and *n*-decane imbibition, respectively. The reduction in liquid imbibition in treated sandstone was greater than for treated carbonate rock, consistent with the contact angles. For example, the increase in static contact angle, advancing contact angle, and receding contact angle of carbonate rock is 81°, 60°, and 110°, respectively, for water, and 95°, 107°, and 90° for *n*-decane. The corresponding values for sandstone are 138°, 95°, and 115° for water, and 104°, 106°, and 43° for *n*-decane. Hence, the maximum difference between contact angles of liquid for treated and untreated sandstone is larger than that obtained for carbonate rock, and therefore, a bigger reduction in liquid imbibition in sandstone is logically expected.

4.4 Effect of Ageing Time in the Nanofluid on Wettability Alteration Efficiency

The effect of different ageing times on liquid imbibition is illustrated in Fig. 11, where a direct relationship between reduction in liquid imbibition and ageing time is evident. The reduction in water imbibition in carbonate rock is 90.0, 95.5, and 95.6 % for 6 h, 1 day, and 6 ageing days, respectively. The corresponding values for *n*-decane are 44.0, 79.1, and 79.2 %, with similar results obtained for sandstone. The reduction in water imbibition in sandstone is 94.9, 96.9, and 97.0 %, and the reduction in *n*-decane imbibition is 89.0, 90.6, and 91.0 % for 6 h, 1 day, and 6 ageing days. According to these data, maximum efficiency of nanofluid is achieved 1 day after application.

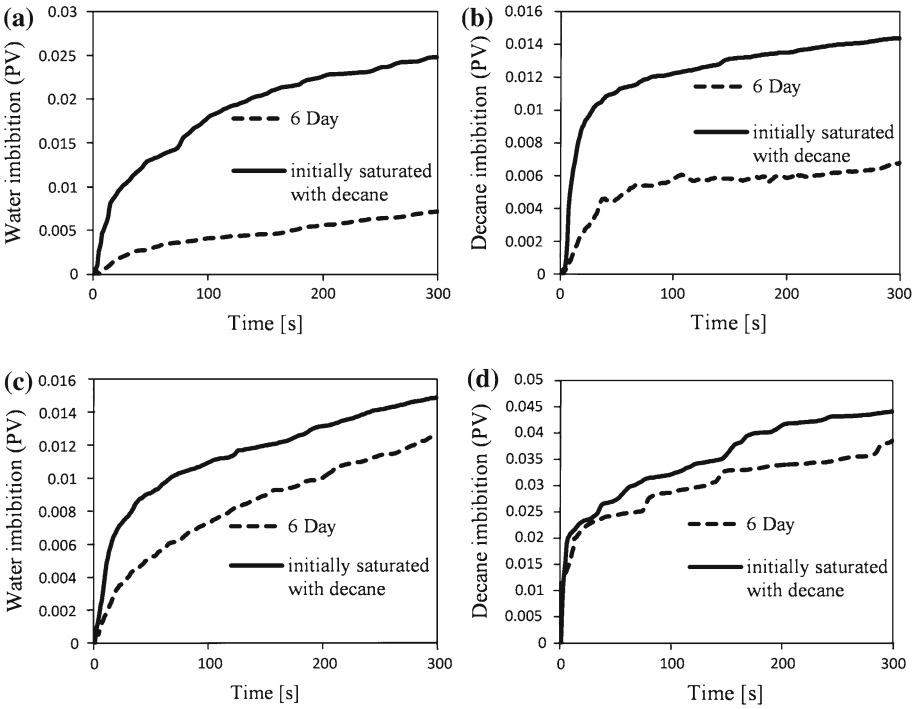

Fig. 12 Imbibition into treated (6 days ageing) rocks not saturated with normal decane and treated rocks initially saturated with normal decane. **a** Water imbibition into carbonate rock, **b** *n*-decane imbibition into carbonate rock, **c** water imbibition into sandstone rock, **d** *n*-decane imbibition into sandstone rock

4.5 Effect of Initial Decane Saturation on Treatment Efficiency

As mentioned earlier, when bottom hole flowing pressure drops below the dew point pressure in gas condensate reservoirs, a liquid saturation of about 60 % could be formed. Consequently, the presence of condensate might affect the treatment efficiency by nanofluid. To find the oil saturation impact, an imbibition test was performed to investigate the effect of initial *n*-decane saturation on the treatment efficiency. Carbonate and sandstone samples were completely saturated with *n*-decane and then treated with nanofluid for evaluation in imbibition tests.

Figure 12 compares the liquid imbibition into treated rocks with and without initial *n*-decane saturation. It shows that liquid imbibition into the initially *n*-decane saturated rock before treatment is slightly more than that of the treated rock not saturated with *n*-decane. The reduction in water and *n*-decane imbibition in carbonate rocks initially saturated with *n*-decane are 83.3 and 55.7 %, respectively. The corresponding values for sandstone initially saturated with *n*-decane are 96.4 and 89.6 %. Therefore, the initial presence of *n*-decane in the rocks slightly decreases the capability of nanofluid for wettability alteration of the rock towards gas wetting.

4.6 Core Displacement Results

As explained previously, brine (2 % KCl) was injected into the air-saturated core at a constant flow rate of 2 cc/min for sandstone rock sample at 70 °C at atmospheric outlet pressure, with the pressure drop across both the untreated and treated cores monitored with time.

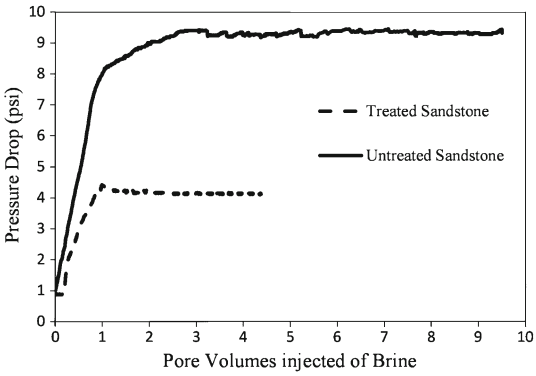

Fig. 13 Pressure drop versus pore volumes injected of brine for untreated and treated sandstone core sample

Figure 13 shows the results for untreated and treated sandstone core. In both cases, the pressure drop increases until a maximum value is reached, after which the pressure drop decreases gradually to a constant value at the steady state. As may be seen, the treated core has a relatively lower pressure drop compared with that of the untreated core, indicating the capability of the nanofluid in changing the wettability from liquid wetting to gas wetting condition. To explain this in a quantitative way, the brine effective permeability at residual gas saturation in treated and untreated cores is calculated from steady-state pressure drop using Darcy's law. It is found that the brine effective permeability at residual gas saturation for an untreated sandstone core is 57 md while the corresponding value for the treated core equals 130 md. The increase in liquid permeability supports the theory that the chemical treatment changes the core surface from preferential water wetting to gas wetting. Also, it should be pointed out that the equality of the contact angles of water and *n*-decane on the treated samples in small slab scale and core scale (after injection of 20 PVs of water to displace the nanofluid) indicates the durability of the chemical treatment at the working temperature.

5 Conclusion

The wettability of carbonate and sandstone rocks is altered from liquid wetting to intermediate gas wetting when treated with nanofluid containing fluorinated chemicals. Basically, a gas wetting surface is achieved by increasing surface roughness and decreasing surface free energy. Nanoparticles develop a nano-structured rough surface, and fluorinated chemicals reduce the surface energy. SEM images and EDX analysis reveal the uniform distribution of fluorine element on the treated rocks, which fact was confirmed by free energy calculation of the surface. The contact angle measurements (static, dynamic, and pseudo-contact angles) demonstrate the capability of the nanofluid in wettability alteration to intermediate gas wetting. The amount of liquid imbibed into the treated rocks decreases significantly compared to untreated ones, indicating the capability of nanofluid in wettability alteration to intermediate gas wetting. Initial saturation of *n*-decane in rocks has a slight effect on treatment efficiency of nanofluid. Thus, a pre-treatment of the rock may be required prior to the application of nanofluid. Core displacement results also indicated that nanofluid could be used for wettability alteration to intermediate gas wetting in reservoir conditions.

Acknowledgments This work is supported by NIOC-R&D (Contract No. 81-88009), which is gratefully acknowledged.

References

Adibhatla, B., Mohanty, K., Berger, P., Lee, C.: Effect of surfactants on wettability of near-wellbore regions of gas reservoirs. J. Pet. Sci. Eng. **52**(1), 227–236 (2006)

Al-Anazi, H., Solares, J.R., Al-Faifi, M.: The impact of condensate blockage and completion fluids on gas productivity in gas-condensate reservoirs. In: SPE Asia Pacific Oil and Gas Conference and Exhibition (2005)

Alzate, G., Franco, C., Restrepo, A., Del Pino Castrillon, J., Barreto Alvares, D., Escobar Murillo, A.: Evaluation of alcohol-based treatments for condensate banking removal. In: International Symposium and Exhibition on Formation Damage Control (2006)

Cassie, A., Baxter, S.: Wettability of porous surfaces. Trans. Faraday Soc. **40**, 546–551 (1944)

Chibowski, E.: Surface free energy of a solid from contact angle hysteresis. Adv. Colloid Interface Sci. **103**(2), 149–172 (2003)

El-Banbi, A., McCain, Jr, W.D., Semmelbeck, M.: Investigation of well productivity in gas-condensate reservoirs. In: SPE/CERI Gas Technology Symposium (2000)

Feng, C., Kong, Y., Jiang, G., Yang, J., Pu, C., Zhang, Y.: Wettability modification of rock cores by fluorinated copolymer emulsion for the enhancement of gas and oil recovery. Appl. Surf. Sci. **258**(18), 7075–7081 (2012)

Hsieh, C.T., Chang, B.S., Lin, J.Y.: Improvement of water and oil repellency on wood substrates by using fluorinated silica nanocoating. Appl. Surf. Sci. **257**(18), 7997–8002 (2011)

Kumar, V., Pope, G., Sharma, M.: Improving the gas and condensate relative permeability using chemical treatments. In: SPE Gas Technology Symposium (2006)

Li, K., Firoozabadi, A.: Experimental study of wettability alteration to preferential gas-wetting in porous media and its effects. SPE Reserv. Eval. Eng. **3**(2), 139–149 (2000a)

Li, K., Firoozabadi, A.: Phenomenological modeling of critical condensate saturation and relative permeabilities in gas/condensate systems. SPE J. **5**(2), 138–147 (2000b)

Li, K., Liu, Y., Zheng, H., Huang, G., Li, G.: Enhanced gas-condensate production by wettability alteration to gas wetness. J. Pet. Sci. Eng. **78**(2), 505–509 (2011)

Li, W., Amirfazli, A.: A thermodynamic approach for determining the contact angle hysteresis for superhydrophobic surfaces. J. Colloid Interface Sci. **292**(1), 195–201 (2005)

Liangui, D., Walker, J., Pope, G., Sharma, M., Peng, W.: Use of solvents to improve the productivity of gas condensate wells. In: SPE Annual Technical Conference and Exhibition (2000)

Muladi, A., Pinczewski, W.: Application of horizontal well in heterogeneity gas condensate reservoir. In: SPE Asia Pacific Oil and Gas Conference and Exhibition (1999)

Noh, M., Firoozabadi, A.: Effect of wettability on high-velocity coefficient in two-phase gas/liquid flow. SPE J. **13**(3), 298–304 (2008)

Sharifzadeh, S., Hassanajili, S., Rahimpour, M.R.: Wettability alteration of gas condensate reservoir rocks to gas wetness by sol–gel process using fluoroalkylsilane. J. Appl. Polym. Sci. **128**(6), 4077–4085 (2013)

Shi, L., Xitan, Z., Zhijian, D., Kai, L., Gang, C., Ning, L.: Investigation of revaporization of retrograde condensate. In: SPE Middle East Oil Show (2001)

Siregar, S., Hagoort, J., Ronde, H.: Nitrogen injection vs. gas cycling in rich retrograde condensate-gas reservoirs. In: International Meeting on Petroleum Engineering (1992)

Smith, L., Yarborough, L.: Equilibrium revaporization of retrograde condensate by dry gas injection. Old SPE J. **8**(1), 87–94 (1968)

Tang, G.Q., Firoozabadi, A.: Relative permeability modification in gas/liquid systems through wettability alteration to intermediate gas wetting. SPE Reserv. Eval. Eng. **5**(6), 427–436 (2002)

Tang, G.Q., Firoozabadi, A.: Wettability alteration to intermediate gas-wetting in porous media at elevated temperatures. Transp. Porous Media **52**(2), 185–211 (2003)

Taylor, R., Coulombe, S., Otanicar, T., Phelan, P., Gunawan, A., Lv, W., Rosengarten, G., Prasher, R., Tyagi, H.: Small particles, big impacts: a review of the diverse applications of nanofluids. J. Appl. Phys. **113**(1), 0113011–01130119 (2013)

Washburn, E.W.: The dynamics of capillary flow. Phys. Rev. **17**(3), 273 (1921)

Wenzel, R.N.: Resistance of solid surfaces to wetting by water. Ind. Eng. Chem. **28**(8), 988–994 (1936)

Whitson, C.H., Fevang, Ø., Yang, T.: Gas condensate PVT—what's really important and why? In: IBC Conference Optimization of Gas Condensate Fields, pp. 28–29. London (1999)

Wu, S., Firoozabadi, A.: Permanent alteration of porous media wettability from liquid-wetting to intermediate gas-wetting. Transp. Porous Media **85**(1), 189–213 (2010)